Transcriptome Profile of Hippocampus in Rats Model of Acute Myocardial Ischemia in Response to Electroacupuncture

Xin Wu
Anhui University of Traditional Chinese Medicine
Chenkai Wang
Anhui University of Traditional Chinese Medicine
Kun Wang
Anhui University of Traditional Chinese Medicine
Shuai Cui
Anhui University of Traditional Chinese Medicine
Shengbing Wu
Anhui University of Traditional Chinese Medicine
Guoqi Zhu
Anhui University of Traditional Chinese Medicine
Meiqi Zhou (meiqizhou77@sina.com)
Anhui University of Traditional Chinese Medicine

Research article

Keywords: transcriptome, electroacupuncture, RNA sequencing, hippocampus, acute myocardial ischemia

Posted Date: June 12th, 2020

DOI: https://doi.org/10.21203/rs.3.rs-34686/v1

Abstract

Background: Electroacupuncture (EA) alleviates acute myocardial ischemia (AMI) by regulating some brain areas, including hippocampus. The locus coeruleus (LC) is the main source of norepinephrine (NE) in the brain, including the hippocampus, and regulates cardiovascular function. The aim of the present work was to assess whether LC mediates the positive effects of EA in AMI by altering gene expression levels in the hippocampus. We addressed this in the present study by hippocampus transcriptome profiling in a rat model of AMI following EA treatment.

Results: Myocardial injury markers (ischemia-modified albumin, homocysteine and lipoprotein-associated phospholipase A2) in the serum were downregulated in EA ($P<0.05$) compared to the M group and upregulated in E+L group ($P<0.05$) compared to E group. RNA sequencing analysis of the hippocampus revealed that the downregulation of 27 genes in M vs S as well as upregulation of 40 genes in M vs S were reversed by EA. These differentially expressed genes, which were validated by quantitative real-time PCR, were enriched in 20 Kyoto Encyclopedia of Genes and Genomes pathways related to glycerolipid, glycerophospholipid, and arachidonic acid metabolism as well asnervous system function (glutamatergic, cholinergic, serotonergic, GABAergic synapses).

Conclusions: LC mediates the beneficial effects of EA on AMI-induced injury may be related to the observed transcriptional regulations in the hippocampus. These results provide molecular-level evidence for the therapeutic efficacy of EA in the treatment of AMI.

Background

The World Health Organization predicts that cardiovascular disease, which includes acute myocardial ischemia (AMI), will be the leading cause of disease-related mortality globally in 2020[1]. There is a close physiologic and pathologic relationship between the cardiovascular and nervous systems, as evidenced by the observation that myocardial injury, can lead to inactivation of neurons in specific brain regions[2].

Electroacupuncture(EA) regulates interactions within neural networks[3, 4] and has been used in the treatment of various diseases, including cardiovascular disorders[5]. There is substantial evidence for the efficacy of EA in the treatment of AMI[6–8]. The limbic system is the highest regulatory center of the autonomic nervous system, which regulates cardiac function. The hippocampus is an important brain structure in the limbic system that is linked to the cardiovascular system via the hypothalamus, solitary bundle nucleus, and medulla oblongata[9]. The proliferation of neurons and astrocytes in the dentate gyrus of the hippocampus was found to be reduced and enhanced, respectively, in spontaneously hypertensive rats[10]. And cognitive dysfunction due to AMI in adult mice was correlated with decreases in reactive gliosis and neurogenesis in the hippocampus[11]. In our previous work, we showed that EA alleviates AMI in the hippocampus via regulation of the autonomic nervous system specifically through the synergistic regulation of the sympathetic and vagus nerves by the hippocampal paraventricular nucleus and solitary tract nucleus, respectively[12–14]. These results suggest that the hippocampus is an

important central brain structure mediating the positive effects of EA following AMI. However, whether other brain regions are also involved, and the molecular changes underlying these effects are unknown.

The locus coeruleus (LC) is the main source of norepinephrine (NE) in the brain, including the hippocampus, and regulates cardiovascular function[15–18]. Noradrenergic projections from the LC are activated upon exposure to noxious stimuli[19] and loss of LC noradrenergic neurons decreases NE levels in the central nervous system (CNS)[20, 21].

We speculated that the LC mediates the positive effects of EA in AMI by altering gene expression levels in the hippocampus. We tested this hypothesis in the present study by RNA sequencing (RNA-seq) analysis of the hippocampus in a rat model of AMI following EA treatment.

Result

EA alleviates AMI

Serum levels of three myocardial injury markers differed between the sham (S), AMI (M), EA (E), and AMI + EA + lesion (E + L) groups,as determined by enzyme-linked immunosorbent assay.The rank order of ischemia-modified albumin (IMA), homocysteine (HCY), and lipoprotein-associated phospholipase A2 (LP-PLA2) transcript levels was M > E + L > E > S. The levels of all three markers were significantly higher in the M group compared to the S group($P < 0.01$) and were lower in Ecomparedto M(($P < 0.01$) (Fig. 1).IMA, HCY, and LP-PLA2 were upregulated in the E + L group compared to the E group($P < 0.05$, $P < 0.01$, $P < 0.05$).

EA alters the levels of active substances in sympathetic neurons

The expression levels of the GAP-43 mRNA were highest in the M group, followed by the M + L group and E group, and were lowest in the S group. Compared with the S group,the expression levels of GAP-43 mRNAwas significantly increased *($P < 0.01$)* in the M group.Compared with the M group, the expression levels of GAP-43 mRNA was significantly decreased($P < 0.05$) in the E group. Compared with the E group,the expression levels of GAP-43 mRNA was significantly increased($P < 0.05$) in the E group. The expression levels of the TH mRNA were highest in the M group, followed by the M + L group and E group, and were lowest in the S group. Compared with the S group, the expression levels of TH mRNA was significantly increased *($P < 0.01$)* in the M group. Compared with the M group, the expression levels of TH mRNA was significantly decreased *($P < 0.01$).* Compared with the E group, the expression levels of TH mRNA was significantly increased*($P < 0.05$).*The rank order of NE transporter (NET) gene expression was S > E > E + L > M.Compared with the S group, the expression levels of NET mRNA was significantly decreased *($P < 0.01$)* in the M group. Compared with the M group, the expression levels of NET mRNA was significantly increased *($P < 0.01$)* in the E group. Compared with the E group, the expression levels of NET mRNA was significantly increased *($P < 0.01$)* in the E + L group (Fig. 2).

Hippocampus transcriptome profiling

Gene expression profiles of the hippocampus were determined by RNA- seq and compared between S, M, E, and E + L groups. After removing unknown bases (N) > 5%, low-quality sequences and reads that were too short, 20.71, 41.44, 20.32 and 20.25 Gb of clean bases were obtained from 152.85, 305.58, 149.33 and 147.57 Mb of raw data for the S, M, E and E + L groups, respectively. The Q30 ≥ 88.03% in all cases, indicating good data quality (Table 1 and Figure S1). The ratio of matched reads in the sequence alignment exceeded 91.78%. In all matched reads, the uniquely mapped reads are more than 86.19%. These results indicate that the sequencing depth was sufficient for analyzing differential gene expression between groups. The threshold for differentially expressed genes (DEGs) was defined as|log 2FC|≥1 and Q value≤0.001. The heat map (EXP > 1) revealed differences in the gene expression profiles of the M and S groups (Fig. 3a) indicating that AMI was associated with significant changes in gene expression in the hippocampus. EA also altered transcript levels, as evidenced by the DEGs between the E and M groups. Additionally, the gene expression profilesof the E and E + L groups differed, suggesting involvement of the LC in mediating the effects of EA in the hippocampus of AMI rats. There were 703 DEGs between the S and M groups, including 391that were up-regulated and 312 that were down-regulated (Table S1). Between the M and E groups, there were 567 DEGs, including 312 and 255 that were up and down-regulated, respectively (Table S2). Of the 473 DEGs between the E group and E + L groups, 141 were up-regulated, and 332 were down-regulated (Fig. 3(b) and Table S3).The Venn diagrams revealed 67common DEGs between M vs S and E vs M, and 254 DEGs common to E vs M and E + L vs E (Fig. 3(c,d)).

Table 1
Summary of RNA sequencing results.

Group	Sample	Raw reads	Clean reads	Q30 (%)	Clean read ratio	Total mapped(%)	Uniquely mapped(%)
S	S1	50946206	45891112	88.41	90.08	91.92	86.57
	S2	50945566	46006896	88.7	90.31	91.85	86.62
	S3	50945984	46231830	88.56	90.75	91.78	86.19
M	M1	49189326	44740580	88.21	90.96	92.14	87.22
	M2	52585260	47687462	91.12	90.69	92.92	87.76
	M3	50945510	46098634	88.66	90.49	92.05	87.03
	M4	50945754	46079410	88.8	90.45	92.15	86.91
	M5	50945670	45660720	88.03	89.63	91.65	86.5
	M6	50945572	46060494	88.14	90.41	92.13	87.01
E	E1	50945274	45632592	88.55	89.57	91.83	86.99
	E2	49188076	44788752	88.97	91.06	92.08	86.97
	E3	49188242	45073502	89.23	91.63	92.39	87.5
E + L	E + L1	49188236	45059832	88.93	91.61	92.15	87.27
	E + L2	49188160	44845222	88.93	91.17	92.08	87.01
	E + L3	49188216	45064528	89.05	91.62	92.39	87.46

Gene Ontology (GO) analysis

GO term enrichment was evaluated to categorize biological processes associated with the identified DEGs (Fig. 4). In the S vs M comparison (Table S1), the DEGs were mostly related to cell adhesion(Col6a5, Itga10, LOC102553715, LOC108348159, Col15a1, Gpnmb, Pcdhb2, LOC108349816, Dscam, Glycam1, Glycam1, Tnr, LOC100910275, Pcdhgb5, LOC108353166, Pcdhgb6, Fbln7, Cdhr1, Prkce, Cx3cr1, Cdh6, Wisp3, Col5a1, LOC103693608, Thbs1, LOC108348121, Pcdhgb4, Dgcr2, Pcdhb21, Pdzd2, Dpp4, Pcdh1, Pcdhgc5 and Cdh4) and ionotropic glutamate receptor signaling pathway(Grid2, Cdk5r1, Grik3, Gria1, Camk2a, Grin3a and Grin2a). In the M vs E comparison (Table S2), the DEGs were primarily associated with ion transport (Scn5a, Best3, Slc5a5, Scn11a, Slc22a2, Slc22a8, Kcnj13, Slco1a5, Atp2b4, Atp2b4, Kcnq1, Lcn2, Kcnf1, Slc24a1, Gabrq, Atp4a, Slc40a1, Hfe, Chrna4, Fxyd6, Tspo, Clic3, Steap1, Slc4a5, Scara5, Trpv4, Gabre, Slc5a11, Slc17a6, Slc38a4, Slc4a2, Cftr, Slc5a7, Kcne2 and Clic6) and neuropeptide signaling (Adcyap1, Nmur2, Crhr1, Tac1, Sstr1, Pnoc, Npsr1, Ntsr1, Ecel1, Penk, Grp, Prlhr, Glp1r, Nmbr). The DEGs between E + L and E groups were mainly related tocilium movement (Ccdc151, Ccdc114, Pih1d3, LOC108349819, Rsph4a, Dnah11, LOC103689994, Hydin and Cfap100) and iontransport (Scn5a, Best3, Slc5a5, Chrna5, Slc22a8, Kcnj13, Slco1a5, Atp2b4, Kcnq1, Grin3b, Kcnf1,

Gabrq, Atp4a, Slc40a1, Hfe, Chrna4, Fxyd6, Tspo, Steap1, Slc4a5, Scara5, Trpv4, Slc17a6, Slc38a4, Slc4a2, Cftr, Kcnk16, Kcne2 and Clic6) (Table S3).

Kyoto Encyclopedia of Genes and Genomes(KEGG) pathway analysis

The functions of DEGs were also investigated by KEGG pathway enrichment analysis (Fig. 3a-d). Of the 67 DEGs at the intersection between M vs S and E vs M(Fig. 5a,b and Table S4) and 254 DEGs common to E vs M and E + L vs E(Fig. 5c,d and Table S5). most were associated with metabolism, including glycerolipid (LOC100911615), glycerophospholipid (Pla2g4f), Arachidonic acid (Cbr1, Pla2g4f) as well as with nervous system function including glutamatergic synapses (Pla2g4f) and long-term potentiation (Pla2g4f). cholinergic (LOC102547029, Slc18a3 and Gng4), serotonergic (LOC102547029, LOC100912642 and Gng4) and GABAergic (LOC102547029, Gng4 and Gabre) and retrograde endocannabinoid signaling (LOC102547029, Gng4 andGabre) (Figure(5b)). Other KEGG pathways that were represented among the DEGs were related tothe immune system functions, including helper T cell 17(Th17) differentiation (RT1-Bb, RT1-Da, RT1-Db1, RT1-Ba), Th1 and Th2 cell differentiation(RT1-Bb, RT1-Da, RT1-Db1 and RT1-Ba) (Fig. 5c) and tometabolism, including ether lipid (Pla2g5, Enpp2 and Pla2g4f) and arachidonic acid (Ephx2, Pla2g5, Cbr1 and Pla2g4f) (Fig. 5d).

Validation of DEGs by qRT-PCR

We validated select genes identified by RNA-seq (LOC103692976, Atp5f1 and LOC100910540) by qRT-PCR (Fig. 6). In comparing group M vs S, LOC103692976 were down-regulated for the most with the normalized expression level were − 8.259136854. Whereas, gene LOC103692976 were up-regulated for the most with the normalized expression level were 7.517556 in comparing group E vs M. In comparing group E vs M, gene LOC100910540 were up-regulated for the most with the normalized expression level were 7.998673649. Whereas, gene LOC100910540 were down-regulated with the normalized expression level were − 7.022411553 in comparing group E + L vs E. In comparing group E + L vs E, gene Atp5f1 were down-regulated with the normalized expression level were − 9.763899547. Where genes Atp5f1 were up-regulated with the normalized expression level were 1.015374966 in comparing group E vs M. These qRT-PCR results were consistent with the RNA-seq data for LOC103692976, Atp5f1, and LOC100910540.

Discussion

EA is generally recommended as a treatment for ischemic heart injury, including AMI[22, 23]. IMA, HCY and LP-PLA2 are markers for AMI[24–26]. In this study, serum levels of these markers were elevated in the M group, but this trend was reversed in the E group, suggesting that EA alleviates AMI. An association between AMI and metabolic activity in the CNS has been reported [2, 27]. And the LC has been shown to regulate cardiovascular activity[28].Our data showed that IMA, HCY, and LP-PLA2 were upregulated in the E + L group compared to the E group, suggesting that LC mediates the beneficial effects of EA on AMI-induced injury.

Autonomic nerves play an important role in regulating cardiac function. and their dysfunction has been implicated in cardiovascular diseases[29]. Narrowing of coronary arteries can lead to increased activity of sympathetic nerves and further constriction of blood vessels, which can exacerbate ischemia[30]. Sympathetic nerve remodeling occurs in ischemic areas of AMI, resulting in the upregulation of TH(a sympathetic nerve marker[31]) and affecting systolic and diastolic heart functions[11, 32]. In this study, TH mRNA level was increased in the myocardial tissue of the M group compared to the S group, in accordance with previous findings[33]. However, TH expression was reduced in the E group compared to the M group, implying that EA suppresses sympathetic excitation. NET is also involved in cardiovascular function and disease[34]. We observed that NET mRNA expression in myocardial tissue was lower in the M group than in the S group, but higher in the E group compared to the M group. GAP-43 is a neuron-specific protein that plays an important role in axon outgrowth in neurons [35]. Following nerve injury GAP-43 is upregulated in regenerating axons, which is positively correlated with sympathetic excitability[31].However, this can aggravate myocardial injury. EA exerts cardio protection by inhibiting sympathetic excitability. The differences in TH, NET and GAP-43 mRNA levels between the E group and E + L groups provide further evidence that the LC contributes to the inhibitory effect of EA on sympathetic excitation.

The hippocampus is a critical brain structure for memory and cognition as well as cardiovascular function. Cognitive deficits have been reported in patients with cardiovascular disease [36–38]and heart failure patients exhibit damage to the hippocampus[39, 40].We previously showed that the mechanism by which acupuncture alleviates AMI-induced damage in the hippocampus is through synergistic action of the paraventricular nucleus, which regulate the sympathetic nerve and the solitary tract nucleus, which regulates the vagus nerve[12–14].

In the present study, we investigated whether the LC is also involved in the effects of EA in AMI. By transcriptome analysis, which revealed clear differences between M and S, E and M, and E + L and E groups (Fig. 3).Moreover, the 67 common DEGs observed in the M vs S and E vs M comparisons and the 254 common DEGs in the E vs M and E + L vs E comparisons indicate that AMI alters gene expression in the hippocampus but that this is reversed by EA via a mechanism involving the LC.

The GO analysis identified specific biological processes that are relevant to the therapeutic effects of EA in the context of AMI. A significant GO term in the comparison of S vs M was the ionotropic glutamate receptor signaling pathway(Table S1). Glutamate is involved in reflex regulation of central vascular function by the nucleus tractus solitarii [41–43]. And AMI is linked to the activation of glutamatergic neurons. Consistent with a role for the CNS in AMI, genes that were differentially expressed between the M and E groups were mostly associated with ion transport and neuropeptide signaling (Table S2). AMI is known to cause abnormal ion transport[44]. Neuropeptide Y is neurotransmitter released by sympathetic nerves[45]. Our data suggest that EA ameliorates AMI by modulating ion transport and the neuropeptide signaling in the hippocampus. The DEGs between the E and E + L groups were related to cilium movement and ion transport. changes in NE concentration have been shown to affect the speed of cilium

movement[46], Thus, the LC may alter the activity of NE neurons in the hippocampus of AMI rats in response to EA.

KEGG pathway enrichment analysis showed that pathways that were most highly represented by the DEGs common to M vs S and E vs M were related to metabolism(including arachidonic acid metabolism) and nervous system function (synapses for specific neurotransmitter types)(Fig. 5a,b).This is in accordance with the reported association between eicosapentaenoic acid and arachidonic acid and cardiovascular disease, and the fact that their ratio is a risk marker for coronary artery disease[47]. Increased activity at excitatory (eg, glutamatergic and cholinergic) synapses has been linked to cardiovascular injury[48–52]. Similarly, serotonergic and GABAergic synapses in the CNS influence cardiovascular activity[53–55]while central cholinergic transmission induces cardiovascular changes in hypertensive rats[56]. Our results demonstrate that the aberrant activity of hippocampal neurons induced by AMI can be at least partly mitigated by EA.Our data showed that the expression of multiple genes was altered by AMI and restored by EA treatment.

Ischemic myocardial injury results in the upregulation and post translational modification of factors involved in cell cycle regulation, such as cyclin-dependent kinase-2[57]. In this study, LOC103692976 level was down and up regulated in the hippocampus in M vs S and E vs M comparisons, respectively. Gene annotation revealed that LOC103692976 is involved in the positive regulation of cyclin-dependent protein serine/threonine kinase. DNA methylation plays a role in the control of neurotransmission[58]. The LOC100910540 gene, which is related to methylation, was up and down-regulated in the E vs M and E + L vs E comparisons, respectively. Glycogen is the main source of energy in the brain[59, 60] and glycogenolysis generates energy for neurons in the form of ATP, NADH and lactate[61]. Atp5f1 was upand down regulated in the E vs M and E + L vs E comparisons, respectively. Atp5f1 is involved in ATP metabolism. Thus, the LC affects energy metabolism in hippocampal neurons in response to EA treatment.

Our study was limited by a small sample size that precluded extensive statistical analyses. Additional studies are therefore needed to clarify the molecular mechanisms underlying the beneficial effects of EA in AMI.

Conclusions

Our data demonstrate that EA is an effective treatment for treat AMI that functions by inhibiting sympathetic activity. We also showed that the LC mediates the positive effects of EA on AMI, possibly via regulation of metabolism and neuro transmissionin the hippocampus. These results provide empirical evidence for the therapeutic efficacy of EA in mitigating tissue injury caused by AMI.

Methods

Animals

Adult Sprague Dawley rats(SPF, male, 180–220 g, 6 weeks)) were obtained from Jinan Pengyue Laboratory Animal breeding Co. Ltd (number of animal license SCXK (Shandong) 20190003)and housed in the ventilated cages with free access to food and water. All animal procedures were conducted in accordance with the Animal Use Guidelines of Anhui University of Chinese Medicine and Anhui Laboratory Animal Center(Approval number:AHUCM-rats-2020002). During the experiment, the pain and discomfort of the animals were minimized and the number of animals was reduced. The rats were randomized to S, M, E and E + L groups. Experiments were performed among 24 rats with six animals per group. The study design is depicted in Fig. 7.

AMI model and EA

The AMI model was established as previously described [14, 62], with some modifications. Briefly, after isoflurane-induced anesthesia(4%), coronary artery ligation was performed on the left anteriorartery in the M, E and E + L groups. A high T wave and J point elevation ≥ 0.1 mV on ECG implied successful establishment of the AMI model. Rats in the S group underwent surgery without arterial ligation. EA stimulation parameters and location have been previously described [14], Specifically, the Shenmen(HT7)-Tongli(HT5) segments were identified relative to the human meridian line. For rats in the E and E + L groups, three sterile electrodes were inserted into these segments. the frequency and voltage of stimulation were set at 2 Hz and 1 mA, respectively. EA treatment was administered for 30 min daily for 3 consecutive days. For rats in the S and M groups, electrodes were inserted but no current was delivered.

LC lesioning

A mixture of rAAV-flex-taCasp3-TEVp-WPRE-pA and rAAV-DBH-CRE viruses[63] was injected into the LC bilaterally at thefollowing coordinates (AP: -9.84 mm, L: 1.4 mm and H: -7 mmfrom Bregma) [64].

Extraction of tissue sampling and RNA-Seq experiment

After three days of EA. rats were sent into a confined euthanasia chamber(size:32 × 25 × 20 cm, Shanghai yuyan scientific instrument co. LTD,Shanghai□China), and then100% CO2 was released into the chamber at the flow rate of 2L/min for 10 min. And the hippocampus was quickly removed and flash frozen in liquid nitrogen and stored at -80◦C until use. Three or six hippocampus tissue samples were obtained from each of the four group (S, M, E, and E + L) for RNA sequencing. Total RNA was isolated using TRIzol reagent (Invitrogen, Carlsbad,CA, USA) according to the manufacturer's protocol. RNA quality was evaluatedwith a Lab-on-chip Model 2100 bioanalyzer (Agilent Technologies, Palo Alto, CA, USA). RNA concentration,purity, and integrity were assessed with a spectrophotometer (Nanodrop Technologies, Wilmington, DE,USA), Qubit® RNA Assay Kit and Qubit® 2.0 Flurometer (Life Technologies, Pleasanton, CA, USA) and Model 2100 bioanalyzer, respectively.RNA-seq libraries were constructed using an NEBNext® Ultra™ RNA Library Prep Kit for Illumina® (New England Biolabs, Ipswich, MA, USA) according to the manufacturer's instructions. The quality of each sample library was determined with a Model 2100 bioanalyzer. The libraries were sequenced and paired-end reads were generated using a BGISEQ-500 platform (Beijing Genomics Institute,Wuhan, China).

Sequence filtering, mapping, and annotation

Raw reads with unknown bases (N) > 5%, low-quality sequences and reads that were too short (less than 16nt) as determined using FASTX-Toolkit (v0.0.13) were discarded. Paired-end clean reads were aligned to the rat reference genome (NCBI assembly Rnor_6.0) using TopHat2[65] with default parameters. The numbers of reads mapped to each gene was counted with HTSeq[66]. Uniquely localized reads were used to calculate reads number and reads per kilobase per million mapped reads value[67] for each gene. The clean reads were assembled into the transcriptome and expression levels were calculated using Cufflinks software (http://cole-trapnell-lab.github.io/cufflinks/). The genes were mapped to the KEGG database (http://www.genome. jp/kegg) using the BLASTx tool with a cut-off e-value of 10 − 5, and the GO database (http://www.geneontology.org/) was used for gene functions annotations with Blast2GO[68].

Analysis of DEGs

DEGs were analyzed using edgeR package[69]. DEGSeq R package v1.20.0[70] was used to evaluate DEGs in the hippocampus of each three ratsper group. Fold change in gene expression was estimated using edgeR. The threshold for significantly differential expression was log2 (fold change) ≧ 1or P-value ≦ 0.01and false discovery rate(FDR) < 0.05.

GO analysis

GO analysis of DEGs was performed using GOseq R package[71], in which the P-value is based on the Poisson exact test. GO terms with corrected P value (FDR) less than 0.05 were considered significantly enriched for a DEG. KEGG pathway enrichment analysis for DEGs and statistical enrichment testing were performed using KOBAS software[72], with a corrected P value less than 0.05 set as the criterion for significant enrichment.

Validation of DEGs by qRT-PCR

Three up-regulated and three down-regulated DEGs identified by RNA-seq were selected for qRT-PCR validation. These genes covered the whole spectrum of differential expression (ie, log2 fold change. from − 9.76 to + 7.99). The QuantiNova SYBR Green PCR kit (Qiagen, Valencia, CA, USA) was used for qRT-PCR, which was performed according to a standard protocol on the Step One Real-Time PCR System (Applied Biosystems, Foster City, CA, USA). The primers used for PCR amplification are shown in Table S6. The reaction conditionswere as follows: denaturation at 95 °C for 1 min, followed by 40 cycles of 95 °C for 15 s and 63 °C for 25 s. Successive qRT-PCR assays were performed with three biological and three technical replicates. To verify product specificity, a melting curve analysis was performed after each amplification. mRNA levels were normalized to that of the housekeeping gene β actin and relative expression level was calculated with the $2^{-\Delta\Delta Ct}$ method[73].

Data analysis

Data are expressed as mean ± standard deviation and were analyzed using SPSS v21.0software (SPSS Inc., Chicago, IL, USA).$P < 0.05$ was considered significant.

Availability of data and materials

The analyzed data sets generated during the present study are available from the corresponding author on reasonable request.

Abbreviations

EA: electroacupuncture LC: locus coeruleus; AMI: acute myocardial ischemia; RNA-seq: RNA sequencing; DEGs: differentially expressed genes; GO: gene ontology; KEGG: kyoto Encyclopedia of Genes and Genomes; NE: norepinephrine; SD:Sprague Dawley; HT7:Shenmen; HT5:Tongli

Declarations

Data analysis

Data are expressed as mean ±standard deviation and were analyzed using SPSS v21.0software (SPSS Inc., Chicago, IL, USA). $P < 0.05$ was considered significant.

Availability of data and materials

The analyzed data sets generated during the present study are available from the corresponding author on reasonable request.

Acknowledgments

We thank the Wuhan Genomics Institute for assistance with experiments.

Funding

The present work was supported by grants from National Natural Science Foundation of China (8167150648), National Basic Research Program of China (973 Program) (2018YFC1704600) and Natural Science Foundation of Anhui Province (1908085MH289). The funders had no role in study design, data collection and analysis, decision to publish, or preparation of the manuscript.

Author information

Affiliations

[1]Graduate School, Anhui University of Chinese Medicine, Hefei 230038, China.

[2]Key Laboratory of Xin'an Medicine, Ministry of Education, Anhui University of Chinese Medicine, Hefei 230038, China.

[3]Research Institute of Acupuncture and Meridian, Anhui University of Chinese Medicine, Hefei 230038, China.

[4]Bozhou Institute of Chinese Medicine, Anhui Academy of Traditional Chinese Medicine, Bozhou 236800,China.

(Xin Wu[1], Chenkai Wang[1], Kun Wang[2], Shuai Cui[3], Shengbing Wu[2],Guoqi Zhu[2] and Meiqi Zhou [3,4*])

Contributions

Project design: MEZ. Experiments and data analysis:XW, CKW, SC, KW, SBW and GQZ. Manuscript preparation:XW and MQZ. Manuscript revision:MQZ. All authors reviewed the results and approved the final version of the manuscript.

Corresponding author

Correspondence to Meiqi Zhou.

Ethics declarations

Ethics approval and consent to participate

The protocol of this research was submitted to and approved by the Institutional Animal Care and Use Committee of Anhui University of Chinese Medicine, China (permit number: (Approval number: AHUCM-rats-2020002).

Consent for publication

Not Applicable.

Competing of Interest

All authors declare no personal or financial conflicts of interest.

References

1. Milani RV, Lavie CJ. Health care 2020: reengineering health care delivery to combat chronic disease. Am J Med. 2015;128(4):337–43.
2. Fiechter M, Roggo A, Haider A, Bengs S, Burger IA, Maredziak M, Portmann A, Treyer V, Becker AS, Messerli M, et al. Metabolic Activity in Central Neural Structures of Patients With Myocardial Injury. Journal of the American Heart Association. 2019;8(19):e013070.
3. Yuanyuan F, Lijun B, Yanshuang R, Hu W, Zhenyu L, Wensheng Z, Jie T. Investigation of the large-scale functional brain networks modulated by acupuncture. Magn Reson Imaging. 2011;29(7):958–65.
4. Hui KK, Marina OClaunch JD. Acupuncture mobilizes the brain's default mode and its anti-correlated network in healthy subjects. Brain Res. 2009;1287:84–103.

5. Jr SF. Acupuncture for cardiovascular disorders. Problems in Veterinary Medicine. 1992;4(1):125.
6. Li P,., Pitsillides KF, Rendig SV, Pan HL, Longhurst JC. Reversal of reflex-induced myocardial ischemia by median nerve stimulation: a feline model of electroacupuncture. Circulation. 1998;97(12):1186–94.
7. Ballegaard S, Meyer CN, Trojaborg W. Acupuncture in angina pectoris: does acupuncture have a specific effect? J Intern Med. 2010;229(4):357–62.
8. Ballegaard S,., Jensen G, Pedersen, Nissen F. VH: Acupuncture in severe, stable angina pectoris: a randomized trial. Acta Medica Scandinavica. 2010;220(4):307–13.
9. Herman JP, Mueller NK. **Role of the ventral subiculum in stress integration**. 174(2):0–224.
10. **Abnormalities of the Hippocampus are Similar in Deoxycorticosterone Acetate-Salt Hypertensive Rats and Spontaneously Hypertensive Rats **. *Journal of Neuroendocrinology* 2006, **18**(6):466–474.
11. **Sympathetic nerve damage and restoration after ischemia-reperfusion injury as assessed by11C-hydroxyephedrine**. *European Journal of Nuclear Medicine and Molecular Imaging*, 43(2):312–318.
12. Wu S, Cao J, Zhang T, Zhou Y, Wang K, Zhu G, Zhou M. Electroacupuncture Ameliorates the Coronary Occlusion Related Tachycardia and Hypotension in Acute Rat Myocardial Ischemia Model: Potential Role of Hippocampus. Evidence-Based Complementary Alternative Medicine. 2015;2015:1–8.
13. Cui S, Wang K, Wu SB, Zhu GQ, Cao J, Zhou YP, Zhou MQ. Electroacupuncture modulates the activity of the hippocampus-nucleus tractus solitarius-vagus nerve pathway to reduce myocardial ischemic injury. Neural regeneration research. 2018;13(9):1609–18.
14. Cui S, Zhou Y, Wu S, Cao J, Zhu G, Zhou M: **Electroacupuncture Improved the Function of Myocardial Ischemia Involved in the Hippocampus-Paraventricular Nucleus-Sympathetic Nerve Pathway**. *Evidence-Based Complementray and Alternative Medicine*,2018,*(2018-1-1)* 2018, **2018**(3):2870676.
15. Miyawaki T, Kawamura H, Mitsubayashi H, Usui W, Yasugi T. Altered basal firing pattern and postactivation inhibition of locus coeruleus neurons in spontaneously hypertensive rats. Neurosci Lett. 1992;137(1):37–40.
16. Mendiguren A, Pineda J. Cannabinoids enhance N-methyl-D-aspartate-induced excitation of locus coeruleus neurons by CB1 receptors in rat brain slices. Neurosci Lett. 2004;363(1):1–5.
17. Szabo ST, Gold MS, Goldberger BA, Pierre B. Effects of sustained gamma-hydroxybutyrate treatments on spontaneous and evoked firing activity of locus coeruleus norepinephrine neurons. Biol Psychiat. 2004;55(9):934–9.
18. Jones BE, Moore RY. Ascending projections of the locus coeruleus in the rat. II. Autoradiographic study. Brain Res. 1977;127(1):25–53.
19. Florin-Lechner SM, Druhan JP, Aston-Jones G, Valentino RJ. Enhanced norepinephrine release in prefrontal cortex with burst stimulation of the locus coeruleus. Brain Res. 1996;742(1–2):89–97.
20. Marien MR, Colpaert FC, Rosenquist AC. Noradrenergic mechanisms in neurodegenerative diseases: a theory. Brain Res Brain Res Rev. 2004;45(1):38–78.

21. Rommelfanger KS, Weinshenker D. Norepinephrine: The redheaded stepchild of Parkinson's disease. Biochem Pharmacol. 2007;74(2):177–90.
22. Tsou MT, Huang C-H, Chiu J-H. **Electroacupuncture on PC6 (Neiguan) Attenuates Ischemia/Reperfusion Injury in Rat Hearts**. *American Journal of Chinese Medicine*, 32(06):951–965.
23. Fu SP, He SY, Xu B, Hu CJ, Lu SF, Shen WX, Huang Y, Hong H, Li Q, Wang N. **Acupuncture Promotes Angiogenesis after Myocardial Ischemia through H3K9 Acetylation Regulation at VEGF Gene**. *Plos One* 2014, 9.
24. Van BE, Dallongeville J, Vicaut E, Degrandsart A, Baulac C, Montalescot G. Ischemia-modified albumin levels predict long-term outcome in patients with acute myocardial infarction. The French Nationwide OPERA study. Am Heart J. 2010;159(4):570–6.
25. Watson KE. Homocysteine lowering and cardiovascular events after acute myocardial infarction. N Engl J Med. 2007;1(2):1578–88.
26. Huang Y, Wu Y, Yang Y, Li W, Lu J, Hu Y. **Lipoprotein-associated phospholipase A2 and oxidized low-density lipoprotein in young patients with acute coronary syndrome in China**. *Sci Rep*, 7(1):16092.
27. Tawakol A, Ishai A, Takx RA, Figueroa AL, Ali A, Kaiser Y, Truong QA, Solomon CJ, Calcagno C, Mani V. **Relation between resting amygdalar activity and cardiovascular events: a longitudinal and cohort study**. *Lancet*, 389(10071):834–845.
28. Miyawaki T, Kawamura H, Mitsubayashi H, Usui W, Yasugi T. **Altered basal firing pattern and postactivation inhibition of locus coeruleus neurons in spontaneously hypertensive rats**. *Neuroscience Letters*, 137(1):37–40.
29. D'Elia E, Pascale A, Marchesi N, Ferrero P, Senni M, Govoni S, Gronda E, Vanoli E. **Novel approaches to the post-myocardial infarction/heart failure neural remodeling**. 2014, 19(5):611–619.
30. Hu H, Xuan Y, Wang Y, Xue M, Suo F, Li X, Cheng W, Li X, Yin J, Liu J. **Targeted NGF siRNA Delivery Attenuates Sympathetic Nerve Sprouting and Deteriorates Cardiac Dysfunction in Rats with Myocardial Infarction**. *PLOS ONE* 2014, 9.
31. Kobayashi K, Morita S, Sawada H, Mizuguchi T, Yamada K, Nagatsu I, Hata T, Watanabe Y, Fujita K, Nagatsu T. **Targeted Disruption of the Tyrosine Hydroxylase Locus Results in Severe Catecholamine Depletion and Perinatal Lethality in Mice**. *Journal of Biological Chemistry*, 270(45):27235–27243.
32. Hall TM, Gordon C, Roy R, Schwenke DO. **Delayed coronary reperfusion is ineffective at impeding the dynamic increase in cardiac efferent sympathetic nerve activity following myocardial ischemia**. *Basic Research in Cardiology*, 111(3):35.
33. Ting C, Meng-Xin C, You-You L, Zhi-Xiong H, Xiu-Chao S, Wei S, You-Hua W, Yue X, Yu-Ming K, Zhen-Jun T. **Aerobic Exercise Inhibits Sympathetic Nerve Sprouting and Restores β-Adrenergic Receptor Balance in Rats with Myocardial Infarction**. *PLoS ONE*, 9(5):e97810-.
34. Schroeder C, Jordan J. Norepinephrine Transporter Function and Human Cardiovascular Disease. American Journal of Physiology Heart Circulatory Physiology. 2012;303(11):H1273.
35. Xu B, Xu H, Cao H, Liu X, Qin C, Zhao Y, Han X, Li H. **Intermedin improves cardiac function and sympathetic neural remodeling in a rat model of post myocardial infarction heart failure**. *Molecular*

Medicine Reports.

36. Vogels RLC, Scheltens P, Schroeder-Tanka JM, Weinstein HC. **Cognitive impairment in heart failure: A systematic review of the literature**. *European Journal of Heart Failure*, 9(5):440–449.
37. Nunes B, Pais J, Garcia R, Magalhaes Z, Granja C, Silva MC. **Cardiac arrest: long-term cognitive and imaging analysis**. 2003, 57(3):287–297.
38. **Relation of Left Ventricular Ejection Fraction to Cognitive Aging (from the Framingham Heart Study)**. 108(9):1346–1351.
39. Woo MA, Kumar R, Macey PM, Fonarow GC, Harper RM. **Brain Injury in Autonomic, Emotional, and Cognitive Regulatory Areas in Patients With Heart Failure**. 15(3):0–223.
40. Masayuki F, Okuchi K, Miyamoto S, Hiramatsu K, Masuda A. Human hippocampal damage after cardiac arrest. Intensive Care Med. 1996;22(S1):94–4.
41. Gordon FJ, Sved AF. Neurotransmitters In Central Cardiovascular Regulation: Glutamate And Gaba. Clinical Experimental Pharmacology Physiology. 2002;29(5–6):522–4.
42. Guyenet GP. **The sympathetic control of blood pressure**. *Nature Reviews Neuroscience*, 7(5):335–346.
43. Sapru HN. Glutamate Circuits In Selected Medullo-Spinal Areas Regulating Cardiovascular Function. Clinical Experimental Pharmacology Physiology. 2002;29(5–6):491–6.
44. Rhee H, Tyler L. **Effects of myocardial ischemia on cardiac contractility and ion transport in working and Langendorff rabbit heart**. 1984, 180(180):477–487.
45. Ekstrand AJ, Cao R, Bjorndahl M, Nystrom S, Jonsson-Rylander A-C, Hassani H, Hallberg B, Nordlander M, Cao Y. **Deletion of neuropeptide Y (NPY) 2 receptor in mice results in blockage of NPY-induced angiogenesis and delayed wound healing**. *Proceedings of the National Academy of Sciences of the United States of America*, 100(10):6033–6038.
46. Maruyama I. **Conflicting effects of noradrenaline on ciliary movement of frog palatine mucosa**. *European Journal of Pharmacology*, 97(3–4):0–245.
47. Toshikazu K, Yasunori U, Takayoshi N, Mitsuru W, Yuki M, Koshi M, Mayu N, Akio H, Mitsutoshi A, Kazunori K. **Relationship between coronary plaque vulnerability and serum n-3/n-6 polyunsaturated fatty acid ratio**. 2011, 75(10):2432–2438.
48. Sved AF, Ito S, Sved JC. **Brainstem mechanisms of hypertension: Role of the rostral ventrolateral medulla**. 5(3):262–268.
49. Wildt DJD, Porsius AJ. **Central cardiovascular effects of physostigmine in the cat; Possible cholinergic aspects of blood pressure regulation**.
50. Giuliano R, Ruggiero D, Morrison S, Ernsberger P, Reis D. **Cholinergic regulation of arterial pressure by the C1 area of the rostral ventrolateral medulla**. *Journal of Neuroscience the Official Journal of the Society for Neuroscience*, 9(3):923–942.
51. Brezenoff HE, Giuliano R. **Cardiovascular Control by Cholinergic Mechanisms in the Central Nervous System**. *Annu Rev Pharmacol Toxicol*, 22(1):341–381.

52. Kubo T, Fukumori R, Kobayashi M, Yamaguchi H: **Altered Cholinergic Mechanisms and Blood Pressure Regulation in the Rostral Ventrolateral Medulla of DOCA-Salt Hypertensive Rats - Identification by microinjection of L-glutamate**. 1998, **45**(3):327–332.
53. Connor HE, Higgins GA. **Cardiovascular effects of 5-HT1A receptor agonists injected into the dorsal raphe nucleus of conscious rats**. *European Journal of Pharmacology*, 182(1):0–72.
54. Nalivaiko E, Sgoifo A. **Central 5-HT receptors in cardiovascular control during stress**. *Neuroscience & Biobehavioral Reviews*, 33(2):95–106.
55. Mendon?A MM, SJ S, dCK R, Danielle I, GP C, Eugene N, FMA P, FR N, PG R. B. CD: **Involvement of GABAergic and Adrenergic Neurotransmissions on Paraventricular Nucleus of Hypothalamus in the Control of Cardiac Function**. *Frontiers in Physiology*, 9:670-.
56. **Central cholinergic activation induces greater thermoregulatory and cardiovascular responses in spontaneously hypertensive than in normotensive rats**.
57. Liem DA, Zhao P, Angelis E, Chan SS, Zhang J, Wang G, Berthet C, Kaldis P, Ping P, MacLellan WR. **Cyclin-dependent kinase 2 signaling regulates myocardial ischemia/reperfusion injury**. *Journal of Molecular & Cellular Cardiology*, 45(5):0–616.
58. Holloway T, González-Maeso J. **Epigenetic Mechanisms of Serotonin Signaling**. *Acs Chemical Neuroscience*, 6(7):1099–1109.
59. Obel LF, Müller MS, Walls AB, Sickmann HM, Bak LK, Waagepetersen HS, Schousboe A. **Brain glycogen—new perspectives on its metabolic function and regulation at the subcellular level**. *Frontiers in Neuroenergetics*, 4.
60. Magistretti PJ. Regulation of glycogenolysis by neurotransmitters in the central nervous system. Diabete Metabolisme. 1988;14(3):237–46.
61. Daniel SCJ, Corrado K, Heikki C, Ls, Henry M, Felix S, Anne-Karine JMP. B-S: **Norepinephrine stimulates glycogenolysis in astrocytes to fuel neurons with lactate**. *PLOS Computational Biology*, 14(8):e1006392-.
62. Sanbe A, Tanonaka K, Hanaoka Y, Katoh T, Takeo S. Regional energy metabolism of failing hearts following myocardial infarction. Journal of Molecular Cellular Cardiology. 1993;25(9):995–1013.
63. Gray DC, Sami M, Wells JA. Activation of specific apoptotic caspases with an engineered small-molecule-activated protease. Cell. 2010;142(4):637–46.
64. Büttner-Ennever J. The Rat Brain in Stereotaxic Coordinates, **3rd edn**. J Anat 1997, 191(Pt 2):315.
65. Daehwan, Kim. Geo, Pertea, Cole, Trapnell, Harold, Pimentel, Ryan, Kelley: **TopHat2: accurate alignment of transcriptomes in the presence of insertions, deletions and gene fusions**.
66. Anders S, Pyl PT, Huber W. **HTSeq—a Python framework to work with high-throughput sequencing data**. 2015, 31(2):166–169.
67. Mortazavi A, Williams BA, McCue K, Schaeffer L, Wold B. Mapping and quantifying mammalian transcriptomes by RNA-SEq. Nature methods. 2008;5(7):621–8.

68. Conesa A, Gotz S, Garcia-Gomez JM, Terol J, Talon M, Robles M. **Blast2GO: a universal tool for annotation, visualization and analysis in functional genomics research**. *Bioinformatics*, 21(18):3674–3676.
69. Robinson MD, McCarthy DJ, Smyth GK. **edgeR: a Bioconductor package for differential expression analysis of digital gene expression data**. *Bioinformatics*, 26(1):139–140.
70. Wang L, Feng Z, Wang X, Wang X, Zhang X. **DEGseq: an R package for identifying differentially expressed genes from RNA-seq data**. 2010, 26(1):136–138.
71. Young MD, Wakefield MJ, Smyth GK, Oshlack A. **Gene ontology analysis for RNA-seq: accounting for selection bias**. 11(2).
72. Mao X, Tao C, Olyarchuk JG, Wei L. Automated genome annotation and pathway identification using the KEGG Orthology (KO) as a controlled vocabulary. Bioinformatics. 2005;21(19):3787–93.
73. Livak K, Schmittgen T. **Analysis of Relative Gene Expression Data Using Real-Time Quantitative PCR and the 2-△△Ct Method**. *Methods* 2000, 25(4).

Figures

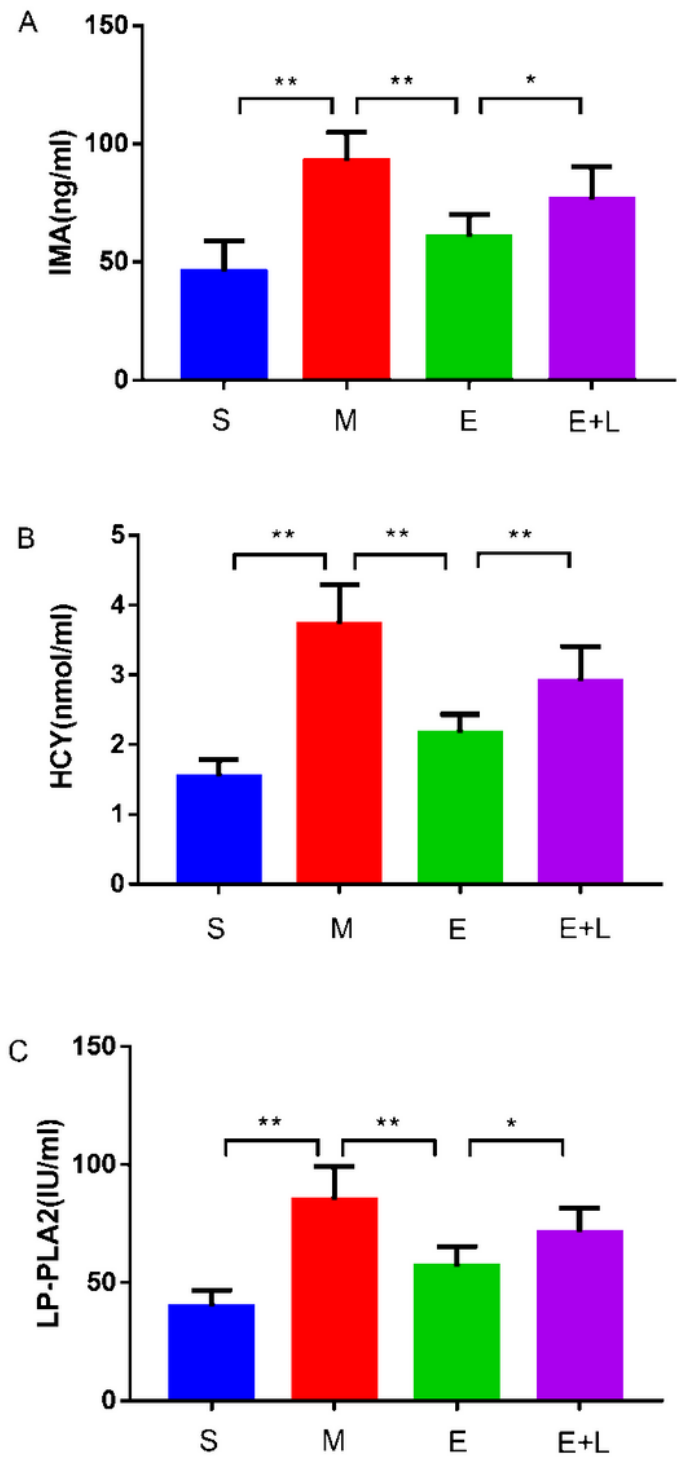

Figure 1

EA induced antimyocardial ischemia like effects. “(a)”show the effect of EA on IMA released into serum. ** p < 0.01,compared with S group, ** p< 0.01, compared with M group, *p< 0.05,compared with E group. “(b)”show the effect of EA on HCY released into serum.** p< 0.01, compared with S group,** p < 0.01, compared with M group,** p < 0.01, compared with E group. “c”show the effect of EA on LP-PLA2

released into serum. **p < 0.01, compared with S group, ** p < 0.01, compared with M group, *p < 0.05, compared with E group.

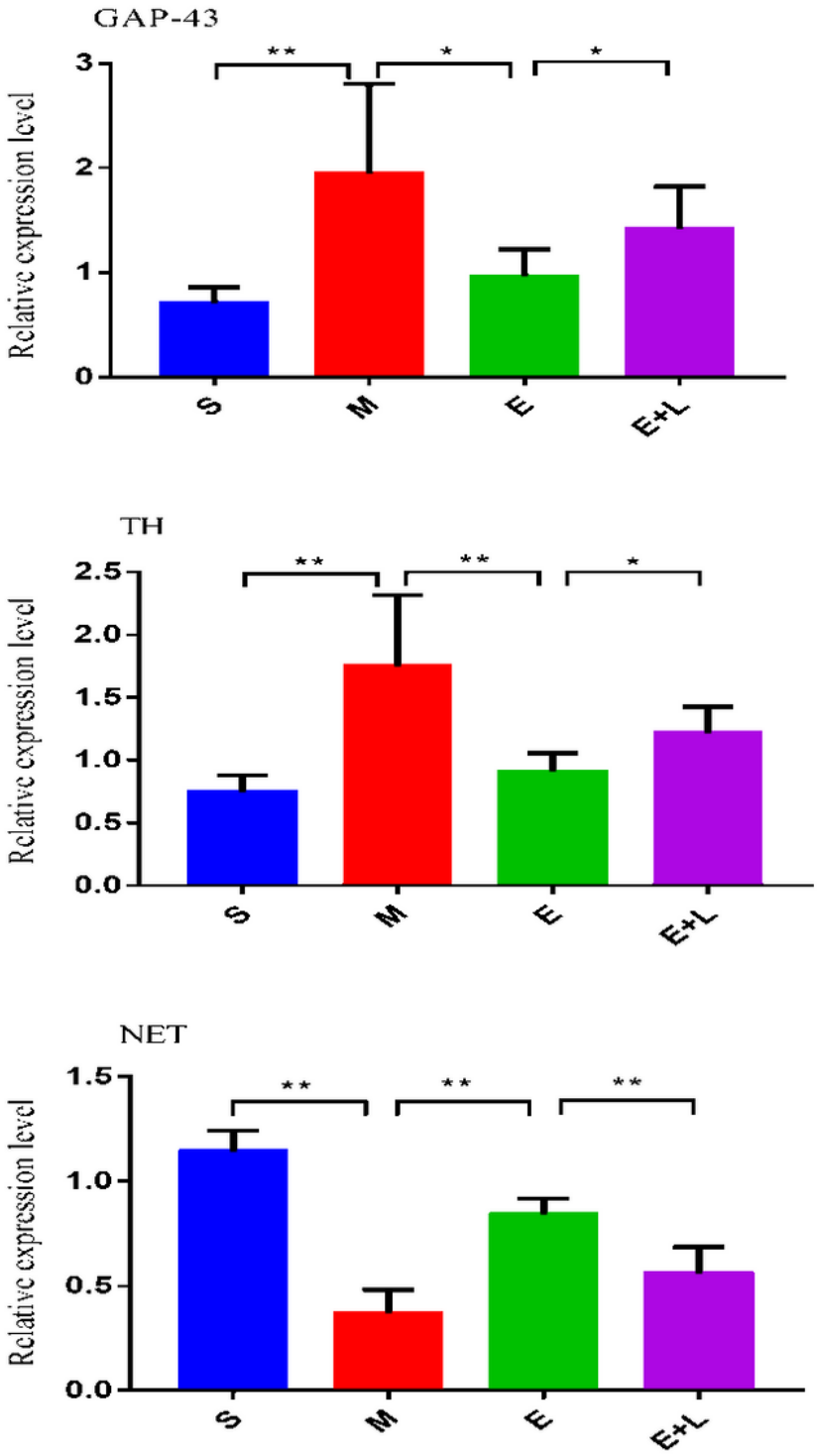

Figure 2

EA alters the levels of sympathetic active substances. “(a)”show the effect of EA on GAP-43 mRNA. ** p < 0.01,compared with S group, * p< 0.05, compared with M group, *p< 0.05,compared with E group. “(b)” show the effect of EA onTH mRNA. ** p< 0.01, compared with S group, ** p< 0.01, compared with M

group, * p < 0.05, compared with E group. “(c)” show the effect of EA on NET mRNA. ** p< 0.01, compared with S group, ** p< 0.01, compared with M group, **p < 0.01, compared with E group.

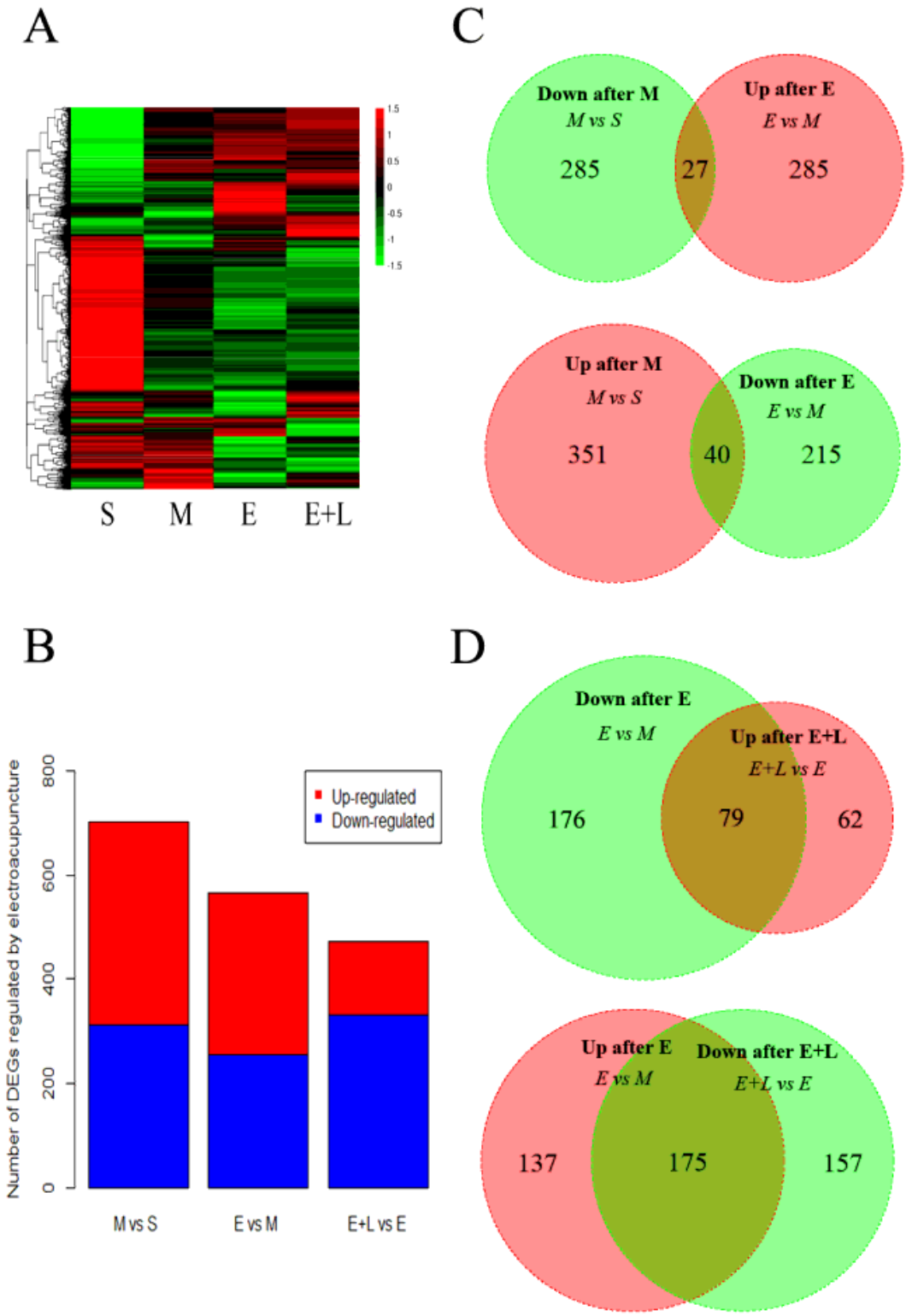

Figure 3

Summary of DEGsanalysis. “(a)” show the Hierarchical clustering. “(b)”show the number of the DEGs. “(c-d)”show the Venn diagrams of common DEGs.

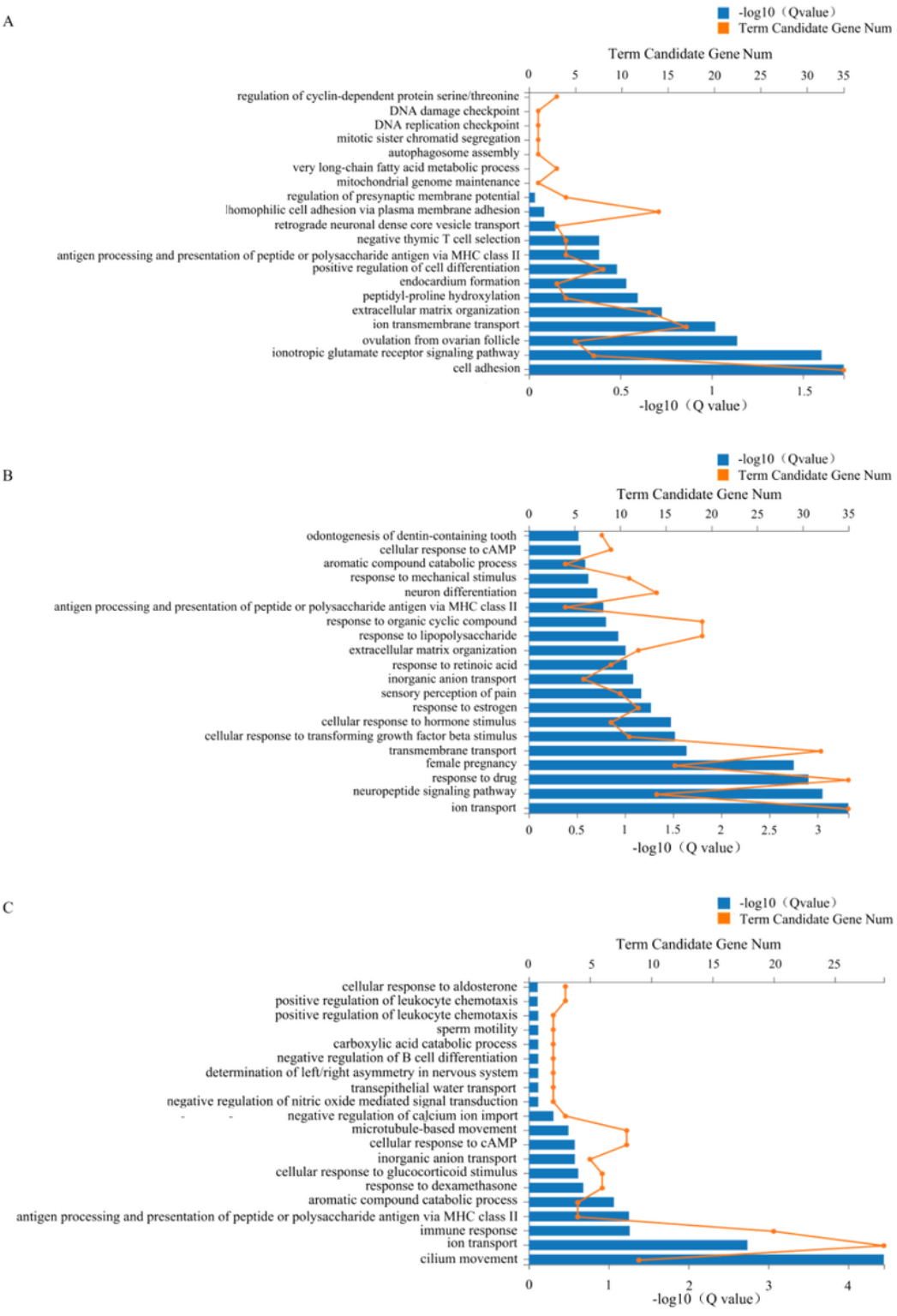

Figure 4

Enriched GO terms of identified DEGs. “(a)” show the GO term of DEGs between M and S group. “(b)” show the GO term of DEGs between E and M group. “(c)” show the GO term of DEGs between E+L and E group.

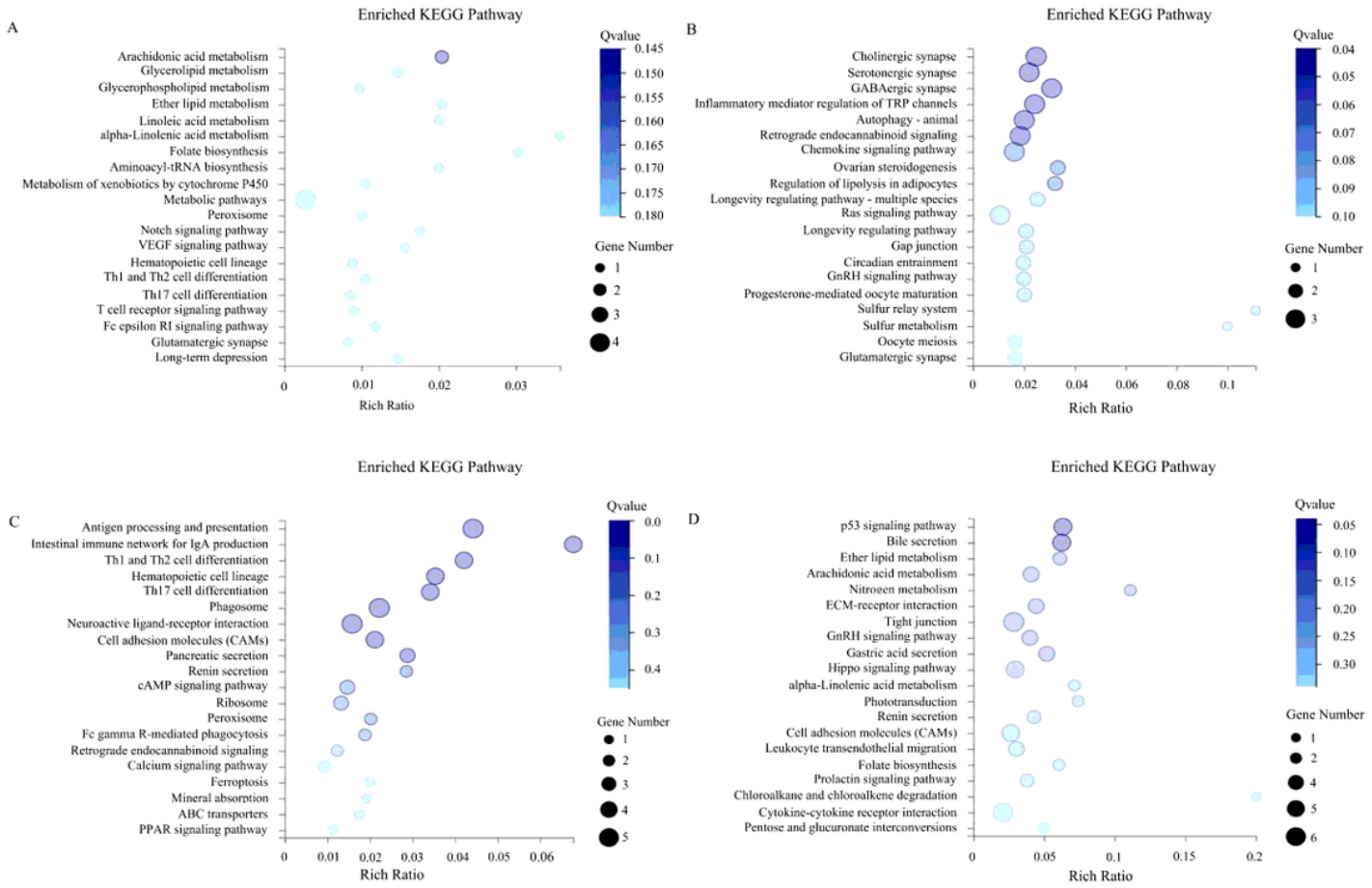

Figure 5

Enriched KEGG pathways of the identified DEGs. (a–d) Pathways of these overlap genes were analyzed using KEGG pathway program, based on overlapped gene numbers shown in Figure 3. “(a)” show the KEGG pathway of DEGs from the 27 genes of Figure 3(c); “(b)” show the KEGG pathway of DEGs from the 40 genes of Figure 3(c); “(c)”show the KEGG pathway of DEGs from the 79 genes of Figure 3(d); “(d)”show the KEGG pathway of DEGs from the 149 genes of Figure 3(d).

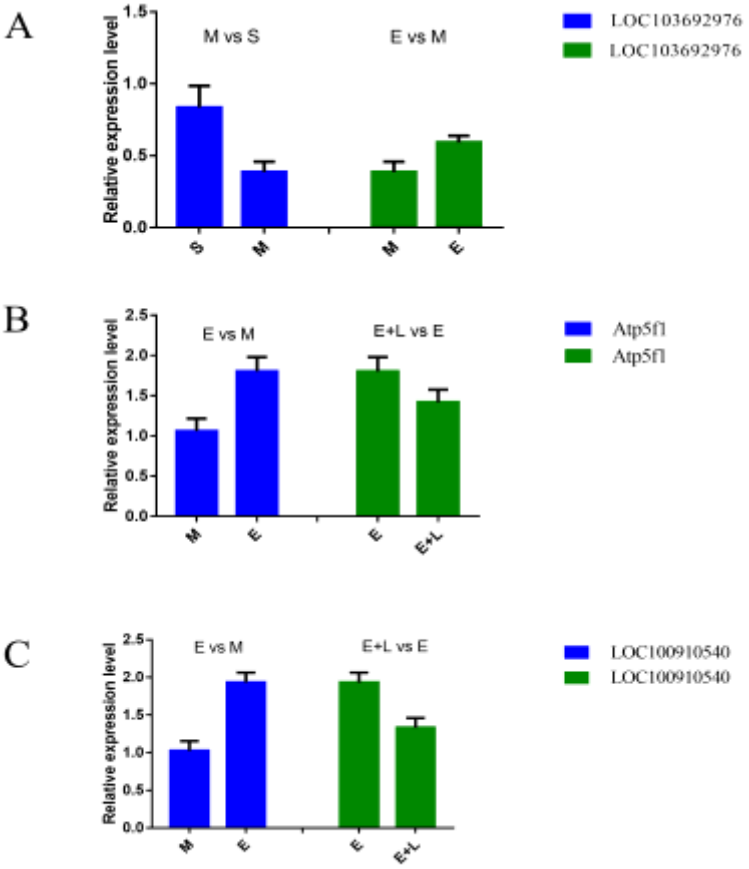

Figure 6

Validation of RNA-seq results for LOC103692976,Atp5f1 andLOC100910540genes by qRT-PCR. (a) LOC103692976 levels in groups S , M and E. (b) Atp5f1 levels in groups M, E and E+L. (c) LOC100910540 levels in groups M, E and E+L. Transcript levels were normalized to that of the housekeeping geneβ-actin, and calculated with the 2-ΔΔCt method. Three biological replicates were analyzed.

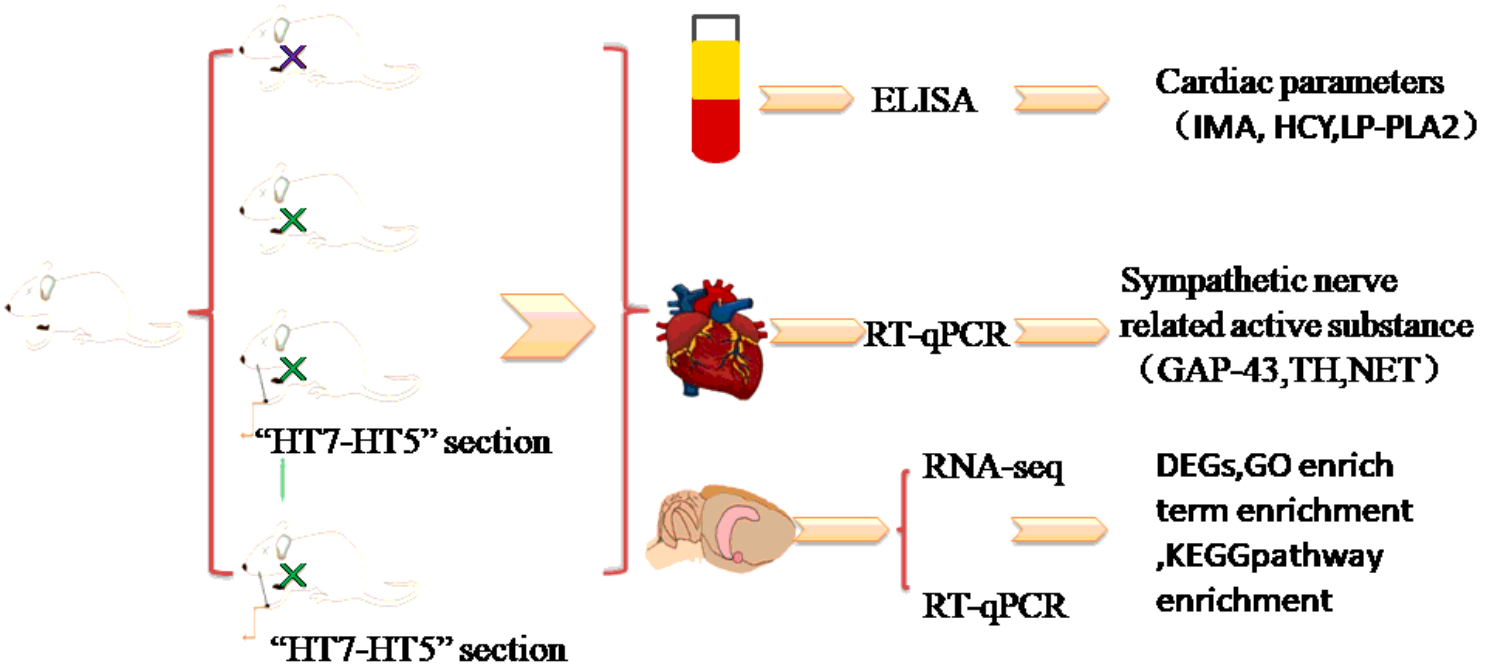

Figure 7

Schematic diagram.